RESEARCH ARTICLE

Distribution and Grain Size Support-Dependent Catalytic Properties of Iridium Nanoparticles

Zahra Amirsardari*, Akram Dourani, Mohamad Ali Amirifar, Nooredin Ghadiri Massoom, Babak Afzali

Space Transportation Research Institute, Iranian space research center, Tehran, Iran

ARTICLE INFO

Article History:
Received 2021-05-15
Accepted 2021-07-11
Published 2021-08-01

Keywords:
Iridium Nanoparticles
Catalyst Support
Catalyst Activity
Grain Size
Decomposition

ABSTRACT

The catalytic reaction of iridium nanoparticles was carried out over gamma-alumina granules to investigate the factors controlling the catalytic activities. The evaluation of iridium nanoparticle activity in the laboratory reactor was done for support grains with different diameter between 1 mm to 4 mm. The characterization of three iridium catalysts was evaluated by XRD, FESEM and EDX before and after catalytic activity. The rate of hydrazine decomposition and hydrogen selectivity increased to 306 h^{-1} and 42% with the better distribution of nanoparticles, regardless of the grain size of catalyst support, whereas the hydrazine decomposition rate was larger for smaller supported catalyst. The probability of hydrazine monohydrate molecules in contact with active sites becomes higher and the movement of reactants and gas products will be easy inside and outside the pores, leading to the increase in reactivity. The rate of the hydrazine monohydrate decomposition and H2 selectivity decreased to 216 h^{-1} and 26% with the lower catalyst grains and the higher size of support along with worse distribution on the surface. The remarkable results of the results prove that support granule size is a dominant factor in the catalytic decomposition.

How to cite this article
Amirsardari Z., Dourani A., Amirifar M.A., Ghadiri Massoom N., Afzali B. Distribution and Grain Size Support-Dependent Catalytic Properties of Iridium Nanoparticles. J. Nanoanalysis., 2021; 8(3): 199-208. DOI: 10.22034/jna.005.

INTRODUCTION

Development of a new route with a low cost method for catalytic reaction is important for widespread applications [1–3]. The use of nanosized metallic particles with high surface area provides a potential system to increase the catalytic activity [4]. Many different nanoparticles have been used for the chemical degradation of fuels and chemical pollutants [5–8]. Hydrazine monohydrate ($N_2H_4{\cdot}H_2O$) with a hydrogen content of 8 wt% is a good hydrogen source for different applications [9,10]. Hydrazine follows two reactive paths of catalytic decomposition for to generate NH_3 and N_2 or H_2 and N_2 [11]. Catalyst and reaction conditions are two important factors affecting the pathways of hydrazine degradation [12–14]. Nobel metals such as iridium nanoparticles are the ideal catalyst for decomposition of hydrazine [15]. The catalytic degradation of hydrazine on nickel-based systems has been investigated as a means of producing hydrogen for on-board or portable applications [16,17]. Despite the extensive research on nickel catalysts, the study of iridium catalysts for decomposition process is still in its infancy.

Iridium nanoparticles are the preferred choice as a catalytically active element for hydrazine decomposition, which possesses high activity and relatively low selectivity towards H_2 generation [18]. The studies of hydrazine decomposition on the Ir(111) surface showed that N-N bond cleavage of hydrazine is more easily accomplished than that of the N-H bond, and the NH_2 radicals can abstract hydrogen atoms one by one from N_2H_4 resulting in the formation of N_2 and NH_3 molecules [19].

In general, many effective routes have been proposed to incorporate catalytic nanoparticles with high performance. Improvement of catalyst support properties such as structure, shape, and type of material composition, typically results in remarkably improved activity and H_2 selectivity [20–22]. A series of lacks for the iridium catalytic decomposition

* Corresponding Author Email: *Z.amirsardari@isrc.ac.ir*

process will inevitably hamper the experimental exploration of high-performance N_2H_4 decomposition catalysts. The researchers showed that the decomposition behaviours of N_2H_4 strongly depend on the support [23]. Although iridium nanoparticle catalysts can accelerate the catalytic activity, the limited surface area of the heterogeneous supported catalysts leads to lower catalytic activity [24–26]. It is clear that the properties of metals depend on the size of their nanoparticles [27–29]. The enormous surface area-to-mass ratio of nanoparticles leads to nanoparticles with extremely high activities for long periods of time under proper conditions that well dispersed these nanoparticles on support granules can exhibit much higher catalytic performance [30–32]. Therefore, it is important to search for a stable support to improve catalytic performance of the catalyst with atomic-sized its good structure [33–36].

There are few experimental results regarding different changes with respect to catalyst reactivity and hydrogen selectivity for iridium nanoparticles. Iridium catalysts have been used widely due to its high activity characteristics for hydrazine decomposition, but there are no experimental results regarding grain size with catalyst reactivity. For different life times (short or long life system), the cost consideration of the catalyst is significant in the operational tests [37]. This catalyst price can be adjusted by controlling the size to prevent nanoparticle loss. Catalytic fabrication with stability and resistance to high operating temperature and pressure conditions is one of the goals of its characterization.

In the present study, three different support grain sizes impregnated with iridium was tested in a lab-scale reactor to investigate the effect on hydrazine monohydrate decomposition rate and hydrogen selectivity by iridium on the γ-alumina catalysts with simple laboratory tools. As a result, the reactivity can be increased by more appropriate distribution of iridium particles on small grain size, and hydrogen selectivity was considerably affected by catalytic support grain sizes. We have, therefore, a very full demonstration that catalyst grain size can affect both activity rate and selectivity of iridium catalytic reactions, and effectively used as a promising catalyst for different application of hydrazine monohydrate.

EXPERIMENTAL

An aqueous solution of dihydrogen hexachloroiridate(IV) hydrate ($H_2IrCl_6.xH_2O$, Sigma-Aldrich) was prepared (20 wt% iridium), and gamma-alumina supports (γ-alumina, grains with 1-2 mm, 2-3 mm, and 3-4 mm diameters, S_{BET}=187-200 m^2g^{-1}) were impregnated three times by this solution at 60°C with 20 percent by weight of metal. The granules were exposed to heat treatment at 80°C for 12 h and then at 400°C for 3 h. Then, the samples were placed in a furnace under hydrogen atmosphere for the reduction process at 400°C for 2 h. The final samples were marked as Ir-1, Ir-2, and Ir-3 for the grain sizes of 1-2 mm, 2-3 mm, and 3-4 mm, respectively.

The catalytic decomposition was initiated by introducing 10 ml hydrazine monohydrate ($N_2H_4{\cdot}H_2O$, Merck) into the self-designed stainless reactor on the 100 mg of granules. The absorption of ammonia is done in a trap containing 1 M HCl, and the volume of nitrogen and hydrogen gases measured via an electronic balance. The TOF value (turnover frequency or the reaction rate, h^{-1}) was calculated in the 80% conversion of $N_2H_4{\cdot}H_2O$ at specific times (t) as follows:

$$TOF=\frac{PV}{3n_{Ir}RTt} \quad (1)$$

where, T, P, and V values are the reaction temperature, the atmospheric pressure, and the volume of generating gases, respectively. R and n_{Ir} are the gas constant and the mole number of iridium.

The phase characterization of the catalysts was plotted using powder X-ray diffraction (XRD, PANalytical X'Pert diffractometer) with Cu Ka radiation. The BET N_2 adsorption–desorption isotherms were measured at 77 K with BELSORP Mini (Microtrac Bel Corp). Scanning electron microscopy was performed using SEM, Tescan Vega3 model, operating at 25 kV. Elemental mapping detection was imaged using an energy dispersive X-ray microanalyzer attached to the SEM.

RESULT AND DISCUSSION

The activity of three different catalytic groups with different sizes was compared for hydrazine monohydrate decomposition. The importance of mass transfer in any specific case depends upon the relative magnitudes of reaction and mass transfer rates between the gas flow and the pore spaces of the catalyst granules. The larger granules can form larger free areas in which gas will move without contact with the catalyst surface. For porous catalysts, the intra-particle diffusion of the reactant

must predominate. The catalytic action will be proportional to the mass of catalyst in small support grains; and in large grains depends on its external surface. Thus, the categories of catalyst sizes for hydrazine monohydrate decomposition cause a difference in the number of granules per gram of catalyst. The images of three categories of iridium catalyst sizes before decomposition tests were shown in Fig. 1. The number of spherical granules at constant weight varies for different support sizes. Therefore, very small support grains of catalyst will be active throughout their volumes, while most of the interior of very large supports grains will be filled with iridium nanoparticles. The probability of hydrazine monohydrate molecules in contact with active sites becomes higher and the movement of reactants and gas products will be easy in and outside the pores, leading to the increase in reactivity.

The XRD patterns obtained from the iridium samples before the hydrogen reduction process can be seen in Fig. 2. The major peaks for IrO_2 are very similar for the three samples, these planes correspond to (1 1 0), (1 0 1) and (2 1 1) at 2θ ~26.5°, 34.4°, and 53.8° with the significant peaks of γ-Al_2O_3 at 2θ ~46° and 68°, respectively. The prepared IrO_2 crystal structure agreed with JCPDS card 15-870 [38]. The average grain sizes of iridium oxide nanoparticles for the Ir-1, Ir-2, and Ir-3 catalysts were calculated from Scherrer's equation to be around 17, 24, and 29 nm by the peak around 34°, respectively. The number of spherical granules at constant weight varies for different support sizes. As expected, the catalyst with grain sizes 1-2 mm, which has more numbers of granules with higher dispersion, has significantly smaller particle size of iridium in comparison to the Ir-3 catalyst. There

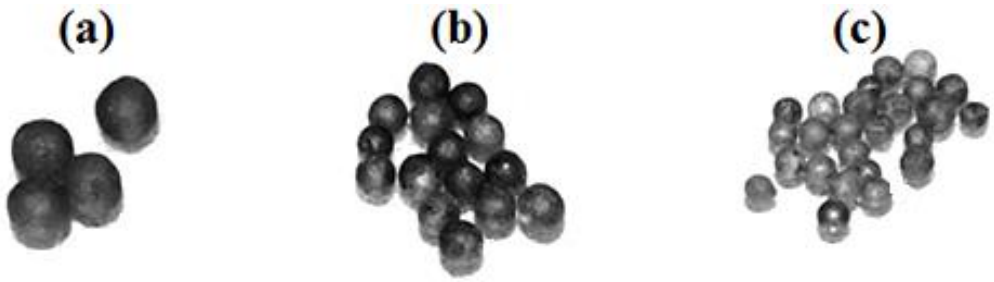

Fig. 1. Catalyst images in three different grain sizes: (a) 3-4 mm, (b) 2-3 mm, and (c) 1-2 mm.

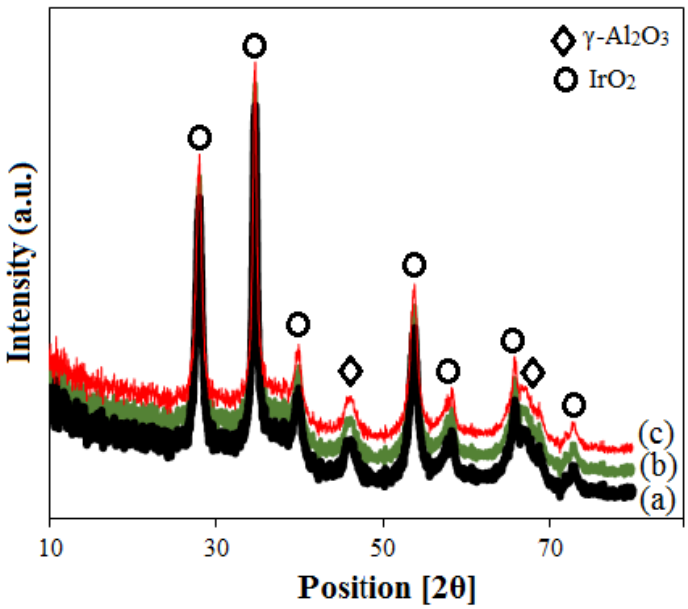

Fig. 2. XRD patterns of iridium catalysts with three different grain sizes: (a) 3-4 mm, (b) 2-3 mm, and (c) 1-2 mm.

will be more surface on Ir-1 with more distance for the iridium particles to disperse and it will prevent the particles from growing and coagulating.

Fig. 3. shows the Ir nanoparticles by SEM images from the surfaces of different support grain sizes. In addition, the performance of scanning electron microscopy/energy dispersive X-ray spectroscopy (SEM/EDX) for accurate mapping determination of the distribution and qualitative elemental analysis of nanoparticles was investigated in Fig. 4. As depicted in Fig. 3a. , the surface of the Ir-3 catalyst shows irregular morphology because the iridium nanoparticles formed by self-aggregation (or intra-particle aggregation) stick together and crystallite size was unclear that the correct size and structure cannot be easily observed from the SEM measurements. The diameter sizes of the Ir-3 catalyst are about 25-31 nm. The morphology of the Ir-2 catalyst was shown in Fig. 3b., spherical structures were obtained in the 22-26 nm diame-

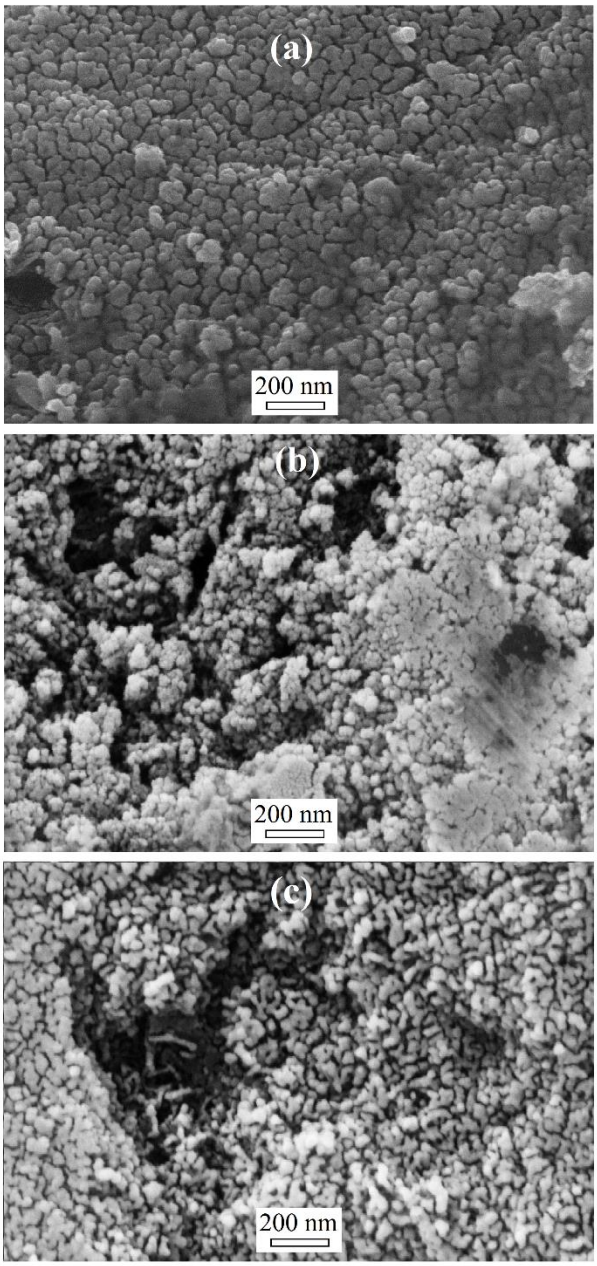

Fig. 3. FESEM image of Ir@γ-alumina surfaces: (a) 3-4 mm, (b) 2-3 mm, and (c) 1-2 mm.

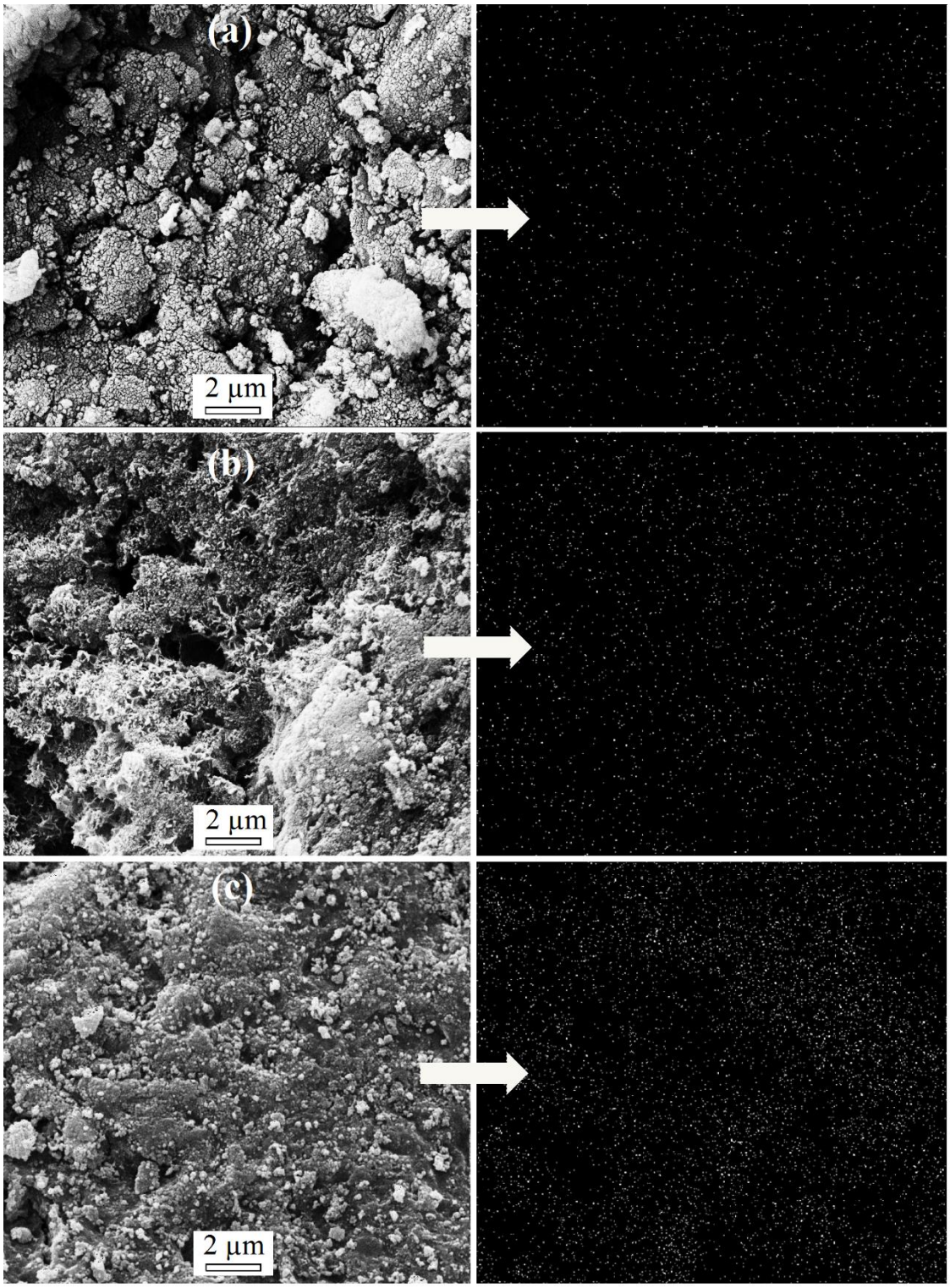

Fig. 4. (left) FESEM image of the iridium catalysts with (right) FESEM elemental mapping images: (a) 3-4 mm, (b) 2-3 mm, and (c) 1-2 mm.

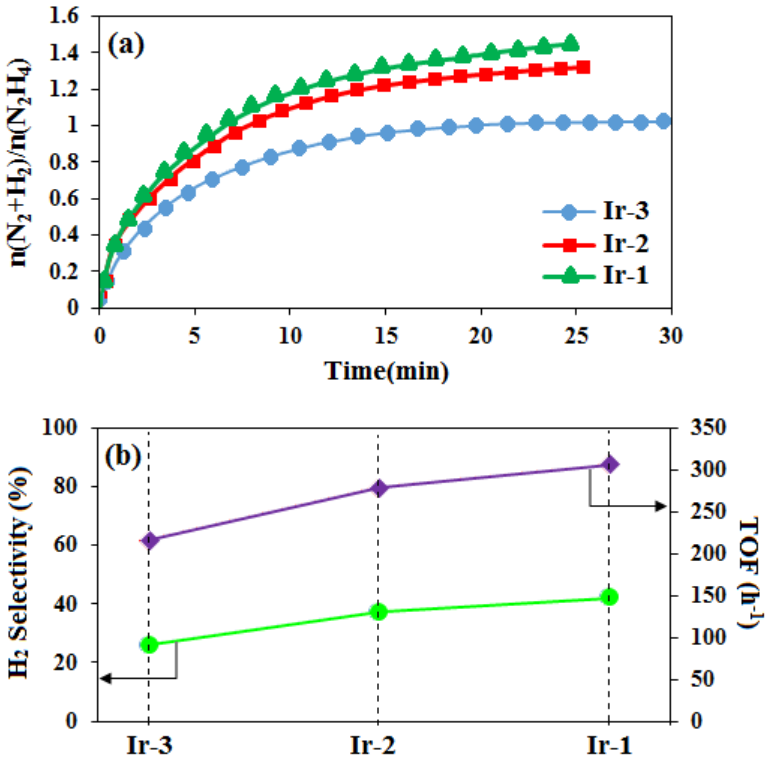

Fig. 5. (a) Volume of the generated gas (H_2 + N_2) versus time, and (b) TOF and H_2 selectivity for the decomposition of hydrous hydrazine catalyzed by iridium@γ-alumina with different support grain sizes.

ter range, but not well dispersed which led to the formation of some flocculates. The nanoparticle aggregation forming on the surface may take place in addition to the typical inter-particle aggregation, producing agglomerates or precipitates that cannot be dispersed as shown in Fig. 3b. In addition, iridium nanoparticles was not homogeneously distributed into the pores as confirmed by SEM-EDX observations (Fig. 4a and b). As the support grain size decreases to approach to 1-2 mm, the division between particles becomes more definite and clearer to show the less inter-particle aggregation during impregnation synthesis. The iridium nanoparticle morphologies turned out to be a different shape of the spheres on the small grain size of support. In the Fig. 4c, no obviously aggregated iridium particles are observed. Elemental mapping images (Fig. 4c) show matched the spatial distribution of iridium, indicating a uniform distribution of Ir on the surface of alumina. Clearly, iridium element is in the whole images with continuous distribution on the alumina spheres. However, these surfaces do not have a homogeneous distribution on spherical granules in agreement with the observations in Fig. 4a and b. But, the iridium nanoparticles in the image of Ir-1 catalyst was are small, seen in all regions with diameter size in a range from 15 to 18 nm. This phenomenon should be related to the shape and surface structure of supports that led to the regular entry of the iridium molecules into the channels or agglomeration into the pores with the free space between the pore entrances. However, the different interaction occurring between iridium and support is probably related to the variation of the surface structures resulting from different distribution of nanoparticles on alumina.

In order to explore the effect of the support grain size on the catalytic performance, the decomposition of hydrous hydrazine catalyzed by iridium samples was carried out under same reaction conditions for all catalysts (Fig. 5a). A preliminary study found that the iridium catalysts possess high catalytic activity towards the decomposition of $N_2H_4 \cdot H_2O$ and the resulting selectivity to H_2 is very low. Our study found that these two parameters for the iridium catalyst can be improved by

grain size of the support. However, upon incorporation of different grain sizes of supports, the iridium catalyst performance can be improved on both catalytic activity and H_2 selectivity. N_2H_4 molecules can be adsorbed on Ir surface accompanied with decomposition through intramolecular or intermolecular reaction. Hydrazine bonds via both N atoms with the N-N axis paralleling to the iridium surface. N-N bond cleavage will facilitate ammonia formation. Hydrazine molecules through exothermic reactions decompose into NH_3, H_2, and N_2 on the iridium catalyst. NH_3 and N_2 are the main gas products at low temperatures, and the H_2 selectivity is low.

It is noted that the N-N bond lengths of N_2H_x (x = 0-4) follow an order of $N_2H_4 > N_2H_3 > N_2H_2 > N_2H > N_2$ at both coverages. This implies that the N-N bond gets strengthened with proceeding the dehydrogenation procedure on Ir(111) surfaces. In addition, except for N_2H, the adsorption strength of the N_2H_x species on the surface decreases with increasing the surface coverage due to the lateral interactions. In the adsorption of NH_3, the site with top energy is preferred with its N atom bonded to surface [39]. As a consequence of the repulsion between the adsorbates, the adsorption of NH_3 becomes weaker with increasing the coverage. But judging from the N-H bond lengths, the NH_3 adsorbate well maintains its gas-phase molecular structure. Three molecules, including NH_2, NH and N bond to the surface via N atom. Obviously, the binding strength between the surface and N increases with the consecutive removal of an H atom from NH_3 [40,41]. For the generated NH_2 radicals from N-N bond cleavage, there exist two possible scenarios. Ammonia is not only a product but also an intermediate. Iridium nanoparticle is an active center for intermediate ammonia decomposition. Decomposition of ammonia is endothermic, and the temperature decreased after this decomposition. The continuation of dissociation extends to NH and H, and the other is the abstraction of an H atom from the vicinity of N_2H_4 in the form of NH_3. It was observed that suitably decreasing the grain size of the iridium catalysts causes increasingly favorable decomposition behavior of $N_2H_4 \cdot H_2O$, and the iridium catalyst reaches its optimal performance at a same composition. Hence, when mass fraction of ammonia starts decreasing, decomposition is more important. Hydrogen and nitrogen gases will increase with hydrazine and ammonia decomposition, and this high pressure of hydrogen causes to inhibit the rate of ammonia decomposition. It has been suggested that the number of catalyst granules increases at smaller grain sizes, and consequently renewal of the active site for reactions enhanced. These mechanisms indicate a strong dependence of the property on the composition.

The dehydrogenation generation from hydrazine over grain sizes 2-3 mm and 1-2 mm under the same reaction conditions completed in 25 min, corresponding to TOF values of 279 h^{-1}, and 306 h^{-1}, respectively. For the Ir-3 catalyst, all of the gas releases from the solution within 30 min. The system using the Ir-3 catalyst showed only around 26% selectivity towards H_2 generation at 25˚C. After 30 min, the reaction rate slowed down and headed to the equilibrium plateau where the reactions were done. The reaction rate per unit mole of active site over the Ir-3 catalyst is 216 h^{-1}, which is inferior to the reported grain size 3-4 mm. In addition, the Ir-1 catalyst is surprising in terms of the selectivity. As seen in Fig. 5b, suitably decreasing the grain size for the Ir-1 and Ir-2 catalysts results in improved H_2 selectivity to 42% and 37%, respectively. As expected, the catalyst with grain sizes 1-2 mm, which has more numbers of granules, could afford more catalytic sites and higher dispersion; has significantly higher catalytic performance in comparison to the Ir-3 catalyst. The product of the decomposition on the Ir-3 creates an impermeable surface layer of the reaction interface which prohibits the reactant come in contact with the catalyst. This does not mean that the inner portions of a large catalyst granule are ineffective, but rather that the inner portions are less effective than the outer portions. As would be expected, the effect is greater at the higher space rates, and at the highest rate, TOF was about 41% greater with the Ir-1 granules than with the regular Ir-3 catalyst. The Ir-2 catalyst showed a somewhat lower gas product than the Ir-1 catalyst, indicating that in this size range some parts of the granules was not readily accessible. Since the Ir-1 catalyst represented the smallest granule size that permitted maximum rate, it may be assumed that the radius of a granule of the median particle size in this range, 1-2 mm, probably is the maximum surface layer thickness effective in the reaction. The effect of the inner portions of the larger granule size on the decomposition reaction was revealed that the reaction values is impacted by the reactant molecules come in contact with the active phase. The reason for this being, the formation of a surface layer composed of producing gas at the catalyst

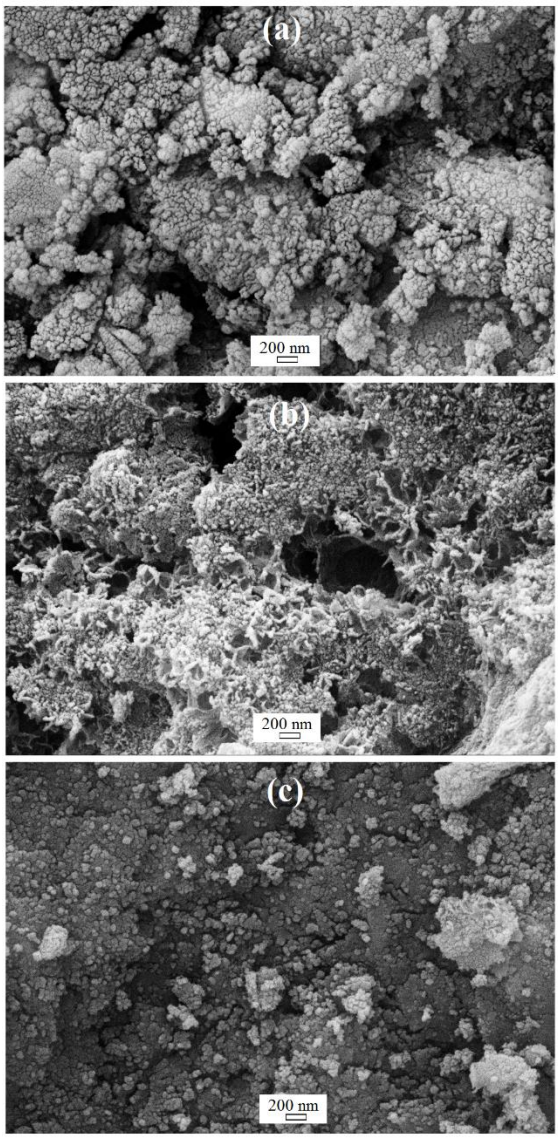

Fig. 6. FESEM image of the Ir@γ-alumina surfaces: (a) 3-4 mm, (b) 2-3 mm, and (c) 1-2 mm after hydrazine monohydrate decomposition.

surface at lower granules, while the probability of hydrazine monohydrate molecules in contact with the active sites of the smaller granule sizes becomes higher and the reactant transportation is found to be easy inside and outside the granule pores, leading to the increase in activity. These observations provide a method for determining the conversions that occurred at different depths in the catalyst pellets. However, iridium nanoparticles would cause a blockage in mesoporous surface, which would weaken the transportation of reactants and products, leading to a lower decomposition rate for larger granules. Meanwhile, iridium nanoparticles would contribute to bigger active sites, which would also exhibit lower reactivity compared with smaller granules with highly dispersed active sites.

To gain insight into the iridium catalytic decomposition of the hydrazine molecules, we conducted microstructure analyses of three samples. The breakage of the carrier was not observed in the conditions of the test, there was an increase of the surface imperfections. The different rate of the gas release at the surface generated different evolutions of the intensity and distribution of the unsteady

temperature profile in the catalyst granules. As seen in Fig. 6., all the three catalyst samples showed tiny nanocrystallites with random orientation are dispersed on the support surface. Compared with the SEM images before decomposition of hydrazine, materials maintained the initial structure after decomposition. Obviously, SEM images exhibited some changes for the Ir-2 and Ir-3 catalysts. Compared with the Ir-1 catalyst, the Ir-2 and Ir-3 catalysts, some aggregations have been observed on the surfaces, especially on the Ir-3 catalyst. These aggregations were supposed to be iridium nanoparticles, which acted as active sites. Distribution of iridium nanoparticles on the small grain size of supports can prevent the aggregation, which lead to improve the transport and the mass diffusion of reactants and products. After impregnation of iridium nanoparticles on the small grain size of supports, the active nanoparticles would sinter on the wall of the alumina spheres stably. Significantly, since each iridium nanoparticle in the hollow cavity was isolated and had a relatively homogeneous environment, the active sites could fully contact with hydrazine reactants and improve the reactivity.

It is a possible reason why these support grain sizes of catalyst exhibit better performance even with lower content of iridium than in other works, providing an economic advantage. To our knowledge, this high performance catalyst provides among the catalystzs containing Ir alone. However, the addition of some nanoparticles, such as nickel, increases performance of the Ir-based catalysts [42–44]. A current challenge was to develop iridium catalysts alone that exhibit good performance, and this work is currently underway.

CONCLUSIONS

The objective of the current work was to study the effect of support grain size from 1 mm to 4 mm on the catalysts activity containing only one phase (iridium nanoparticles) for hydrazine monohydrate decomposition. It is clearly concluded that the TOF and the released hydrogen values mainly depend upon the grain size of the support. Three different catalysts synthesized with the same amount of active phase (20 wt%) showed various sizes of iridium nanoparticles from 17 nm to 29 nm , activities and the trend followed in their released gas patterns is not similar to the profound effect of grain size of the support on the decomposition reaction of hydrazine monohydrate. On the other hand, the decomposition reaction was remarkably hindered from 306 h^{-1} to 216 h^{-1} in the larger grain size, due to less available surface of support in the catalysts with larger iridium nanoparticles.

CONFLICT OF INTEREST

All authors declare that no conflicts of interest exist for the publication of this manuscript.

REFERENCES

1. Delpeux S, Szostak K, Frackowiak E, Bonnamy S, Béguin F. High Yield of Pure Multiwalled Carbon Nanotubes from the Catalytic Decomposition of Acetylene on in Situ Formed Cobalt Nanoparticles. Journal of Nanoscience and Nanotechnology. 2002;2(5):481-4.
2. Wang L-S, Deng J-C, Yang F, Chen T. Preparation and catalytic properties of Ag/CuO nano-composites via a new method. Materials Chemistry and Physics. 2008;108(2-3):165-9.
3. Dominguez A, Fidalgo B, Fernandez Y, Pis J, Menendez J. Microwave-assisted catalytic decomposition of methane over activated carbon for CO2CO2-free hydrogen production. International Journal of Hydrogen Energy. 2007;32(18):4792-9.
4. Zhang J, Chaker M, Ma D. Pulsed laser ablation based synthesis of colloidal metal nanoparticles for catalytic applications. Journal of Colloid and Interface Science. 2017;489:138-49.
5. Shokri A. Degradation of 4-Nitrophenol from industerial wastewater by nano catalytic Ozonation. Int J Nano Dimens 2016;7:160–7.
6. Shokri A. Degradation of Terphetalic Acid from Petrochemical Wastewater by Ozonation and O3/ZnO Processes in Semi Batch Reactor. Archives of Hygiene Sciences. 2017;6(4):348-55.
7. Shokri A, Mahanpoor K. Degradation of ortho-toluidine from aqueous solution by the TiO2/O3 process. International Journal of Industrial Chemistry. 2016;8(1):101-8.
8. Saghi M, Shokri A, Arastehnodeh A, Khazaeinejad M, Nozari A. The photo degradation of methyl red in aqueous solutions by α-Fe_2O_3/SiO_2 nano photocatalyst. J Nanoanalysis 2018;5:163–70.
9. Tafreshi SS, Roldan A, de Leeuw NH. Micro-kinetic simulations of the catalytic decomposition of hydrazine on the Cu(111) surface. Faraday Discussions. 2017;197:41-57.
10. Yao Q, Chen X, Lu Z-H. Catalytic Dehydrogenation of NH_3BH_3, N_2H_4, and $N_2H_4BH_3$ for Chemical Hydrogen Storage. Energy and Environment Focus. 2014;3(3):236-45.
11. Cheng Y, Wu X, Xu H. Catalytic decomposition of hydrous hydrazine for hydrogen production. Sustainable Energy & Fuels. 2019;3(2):343-65.
12. Dai H, Zhong Y, Wang P. Hydrogen generation from decomposition of hydrous hydrazine over Ni-Ir/CeO 2 catalyst. Progress in Natural Science: Materials International. 2017;27(1):121-5.
13. Yao Q, He M, Hong X, Chen X, Feng G, Lu Z-H. Hydrogen production via selective dehydrogenation of hydrazine borane and hydrous hydrazine over MoOx-promoted Rh catalyst. International Journal of Hydrogen Energy. 2019;44(53):28430-40.
14. Xu T-T, Zhang J, Song J-M, Niu H-L, Mao C-J, Zhang S-Y, et al. Synthesis of ZnO-loaded Co0.85Se nanocomposites and their enhanced performance for decomposition of hydrazine hydrate and catalytic hydrogenation of p-nitrophenol.

Applied Catalysis A: General. 2016;515:83-90.
15. Ali I, AlGhamdi K, Al-Wadaani FT. Advances in iridium nano catalyst preparation, characterization and applications. Journal of Molecular Liquids. 2019;280:274-84.
16. Wang Z, Xu L, Huang F, Qu L, Li J, Owusu KA, et al. Copper–Nickel Nitride Nanosheets as Efficient Bifunctional Catalysts for Hydrazine-Assisted Electrolytic Hydrogen Production. Advanced Energy Materials. 2019;9(21):1900390.
17. Singh SK, Lu Z-H, Xu Q. Temperature-Induced Enhancement of Catalytic Performance in Selective Hydrogen Generation from Hydrous Hydrazine with Ni-Based Nanocatalysts for Chemical Hydrogen Storage. European Journal of Inorganic Chemistry. 2011;2011(14):2232-7.
18. Amirsardari Z, Dourani A, Amirifar MA, Massoom NG, Jahannama MR. Controlled attachment of ultrafine iridium nanoparticles on mesoporous aluminosilicate granules with carbon nanotubes and acetyl acetone. Materials Chemistry and Physics. 2020;239:122015.
19. He L, Liang B, Huang Y, Zhang T. Design strategies of highly selective nickel catalysts for H2 production via hydrous hydrazine decomposition: a review. National Science Review. 2017;5(3):356-64.
20. Chen B, Gsalla A, Gaur A, Lui YH, Tang X, Geder J, et al. Porous Wood Monoliths Decorated with Platinum Nano-Urchins as Catalysts for Underwater Micro-Vehicle Propulsion via H_2O_2 Decomposition. ACS Appl Nano Mater 2019;2:4143–9.
21. Wen H, Gan L-Y, Dai H-B, Wen X-P, Wu L-S, Wu H, et al. In situ grown Ni phosphide nanowire array on Ni foam as a high-performance catalyst for hydrazine electrooxidation. Applied Catalysis B: Environmental. 2019;241:292-8.
22. Santos J. Catalytic Decomposition of Hydrazine on Tungsten Carbide: The Influence of Adsorbed Oxygen. Journal of Catalysis. 2002;210(1):1-6.
23. Amirsardari Z, Dourani A, Amirifar MA, Ghadiri Massoom N, Ehsani R. Development of novel supported iridium nanocatalysts for special catalytic beds. Journal of Nanostructure in Chemistry. 2019;10(1):47-53.
24. Vieira R, Bernhardt P, Ledoux M-J, Pham-Huu C. Performance comparison of Ir/CNF and Ir/Al2O3 catalysts in a 2 N hydrazine microthruster. Catalysis Letters. 2005;99(3-4):177-80.
25. Prasad V, Vasanthkumar MS. Iridium-decorated multiwall carbon nanotubes and its catalytic activity with Shell 405 in hydrazine decomposition. Journal of Nanoparticle Research. 2015;17(10).
26. Shim JH, Kim JE, Cho Y-B, Lee C, Lee Y. Oxidation-state dependent electrocatalytic activity of iridium nanoparticles supported on graphene nanosheets. Physical Chemistry Chemical Physics. 2013;15(37):15365.
27. Amirsardari Z, Aghdam RM, Salavati-Niasari M, Shakhesi S. Facile Carbothermal Reduction Synthesis of ZrB2Nanoparticles: The Effect of Starting Precursors. Materials and Manufacturing Processes. 2015;31(2):134-40.
28. Amirsardari Z, Aghdam RM, Salavati-Niasari M, Jahannama MR. The Effect of Starting Precursors on Size and Shape Modification of ZrB_2 Ceramic Nanoparticles. Journal of Nanoscience and Nanotechnology. 2015;15(12):10017-21.
29. Amirsardari Z, Aghdam RM, Salavati-Niasari M, Shakhesi S. Preparation and characterization of a novel hetero-nanostructure of zirconium diboride nanoparticle-coated multi-walled carbon nanotubes. RSC Adv. 2014;4(106):61409-14.
30. Vieira R, Ledoux M-J, Pham-Huu C. Synthesis and characterisation of carbon nanofibres with macroscopic shaping formed by catalytic decomposition of C2H6/H2 over nickel catalyst. Applied Catalysis A: General. 2004;274(1-2):1-8.
31. Kim YH, Kim GH, Kim MS, Jung S-D. Iridium Oxide–Electrodeposited Nanoporous Gold Multielectrode Array with Enhanced Stimulus Efficacy. Nano Letters. 2016;16(11):7163-8.
32. Zhao XG, Huang LQ. Iridium, carbon and nitrogen multiple-doped TiO 2 Nanoparticles with enhanced photocatalytic activity. Ceramics International. 2017;43(5):3975-80.
33. Zhou P, Meng H, Zhang Z, Chen C, Lu Y, Cao J, et al. Stable layered Ni-rich LiNi0.9Co0.07Al0.03O2 microspheres assembled with nanoparticles as high-performance cathode materials for lithium-ion batteries. Journal of Materials Chemistry A. 2017;5(6):2724-31.
34. Chen Z, Jia D-S, Zhou Y, Hao J, Liang Y, Cui Z-M, et al. In situ generation of highly dispersed metal nanoparticles on two-dimensional layered SiO2 by topotactic structure conversion and their superior catalytic activity. Applied Surface Science. 2018;434:1137-43.
35. Wan C, Sun L, Xu L, Cheng D-g, Chen F, Zhan X, et al. Novel NiPt alloy nanoparticle decorated 2D layered g-C3N4 nanosheets: a highly efficient catalyst for hydrogen generation from hydrous hydrazine. Journal of Materials Chemistry A. 2019;7(15):8798-804.
36. Zhang J, Wan L, Liu L, Deng Y, Zhong C, Hu W. PdPt bimetallic nanoparticles enabled by shape control with halide ions and their enhanced catalytic activities. Nanoscale. 2016;8(7):3962-72.
37.Amirsardari Z, Dourani A, Amirifar MA, Massoom NG, Ehsani R, Ghanbarnejad R. Comparative Characterization of Iridium Loading on Catalyst Assessment under Different Conditions. Int J Miner Metall Mater 2020. doi:https://doi.org/10.1007/s12613-020-2058-4.
38. Chen R-S, Chang H-M, Huang Y-S, Tsai D-S, Chiu K-C. Morphological evolution of the self-assembled IrO2 one-dimensional nanocrystals. Nanotechnology. 2004;16(1):93-7.
39. Zhang P-X, Wang Y-G, Huang Y-Q, Zhang T, Wu G-S, Li J. Density functional theory investigations on the catalytic mechanisms of hydrazine decompositions on Ir(111). Catalysis Today. 2011;165(1):80-8.
40. Huang W, Lai W, Xie D. First-principles study of decomposition of NH3 on Ir(100). Surface Science. 2008;602(6):1288-94.
41.Choudhary T V, Santra AK, Sivadinarayana C, Min BK, Yi C-W, Davis K, et al. Ammonia decomposition on Ir (100): from ultrahigh vacuum to elevated pressures. Catal Letters 2001;77:1–5.
42. Zhao P, Cao N, Su J, Luo W, Cheng G. NiIr Nanoparticles Immobilized on the Pores of MIL-101 as Highly Efficient Catalyst toward Hydrogen Generation from Hydrous Hydrazine. ACS Sustainable Chemistry & Engineering. 2015;3(6):1086-93.
43. He L, Huang Y, Liu XY, Li L, Wang A, Wang X, et al. Structural and catalytic properties of supported Ni–Ir alloy catalysts for H2 generation via hydrous hydrazine decomposition. Applied Catalysis B: Environmental. 2014;147:779-88.
44. Hong X, Yao Q, Huang M, Du H, Lu Z-H. Bimetallic NiIr nanoparticles supported on lanthanum oxy-carbonate as highly efficient catalysts for hydrogen evolution from hydrazine borane and hydrazine. Inorganic Chemistry Frontiers. 2019;6(9):2271-8.